https://doi.org/10.1016/j.enggeo.2020.105544

Effects of soil structure on thermal softening of yield stress

Authors: Q. Cheng, C. Zhou*, C. W. W. Ng and C. S. Tang

*Corresponding author

Information of the authors

First author: Dr Q. Cheng

Assistant Professor, School of Earth Sciences and Engineering, Nanjing University, 163 Xianlin Avenue, Nanjing, China

E-mail: chengqing@nju.edu.cn

Co-author: Dr C. Zhou

Assistant Professor, Department of Civil and Environmental Engineering, the Hong Kong Polytechnic University, Hung Hom, Kowloon, Hong Kong

E-mail: c.zhou@polyu.edu.hk

Co-author: Prof. C. W. W. Ng

CLP Holdings Professor of Sustainability, Department of Civil and Environmental Engineering, the Hong Kong University of Science and Technology, Kowloon, Hong Kong

E-mail: cecwwng@ust.hk

Co-author: Prof. C. S. Tang

Professor, School of Earth Sciences and Engineering, Nanjing University, 163 Xianlin Avenue, Nanjing, China

E-mail: tangchaosheng@nju.edu.cn

ABSTRACT

Thermal softening is generally referred as the reduction of yield stress with increasing temperature. Previous experimental studies of thermal softening focus on a single type of specimen (either intact or recompacted). In this study, thermal softening of saturated intact, recompacted and reconstituted loess specimens was investigated through temperature-controlled isotropic compression tests. Scanning electron microscope (SEM) measurements were also carried out to evaluate the microstructures of these specimens. It is found when soil temperature increases from 5 to 50°C, the yield stresses of the intact, recompacted and reconstituted specimens decreased by about 33%, 46% and 51%, respectively. The most resistant structure of intact specimen to thermal softening is mainly because its inter-particle contacts are stabilized by clay aggregates, as evident by SEM results. Reconstituted specimen has the least resistant structure to thermal softening, mainly because clay particles in reconstituted specimen float on the surface of silt particles rather than at inter-particle contacts.

Keywords: yielding; temperature; structure; loess

1. Introduction

In many geological and geotechnical engineering projects such as the landfill cover system, pipeline engineering, geothermal energy development and pavement engineering, soils are always encountered in non-isothermal conditions (Gens, 2010). Temperature has a significant influence on the yielding behaviour of soils. Thermal effects on yield stress of soils have been widely investigated through temperature-controlled compression tests (Tidfors and Sällfors, 1989; Cekerevac and Laloui, 2004; Tang et al., 2008; Di Donna and Laloui, 2015). It is generally found that yield stress decreases with an increase in temperature (i.e., thermal softening of yield stress). In practice, both intact and compacted soils are commonly used as construction materials. During compaction, the initial structure of intact soil is altered. For soil specimens with various soil structures induced by different specimen preparation methods, the thermo-mechanical behaviours are different. For example, Ng et al. (2018) found that under the same thermal load, plastic contractive strain of reconstituted loess is larger than those of intact and recompacted loess. Since no data on thermal softening of yield stress of intact, recompacted and reconstituted loess are reported, the observed effects of soil structure on thermally induced volume change cannot be compared and interpreted within an elastoplastic framework. Some constitutive models have been recently developed to consider the effects of soil structure and overconsolidation on the thermal behaviour of geomaterials (Xiong et al., 2018; Zhou and Ng, 2018). Their capabilities of simulating effects of soil structure on thermal softening of yield stress have not been fully verified.

Soil structure is defined as the arrangement of solid parts of soil and the arrangement of soil pores (Marshall and Holmes, 1979). Following this definition, soil structure can be described by analysing the arrangement of particles, aggregates and their contacts as well as distribution of soil pores and pore

connectivity (Delage et al., 1996; Mitchell and Soga, 2005; Romero and Simms, 2008). The arrangements of particles, aggregates and the contacts between particles/ aggregates can be obtained from scanning electron microscope (SEM) images. Although the distribution of soil pores and pore connectivity cannot be easily quantified, SEM technique is an effective qualitative method and has been widely adopted for soil structure investigation.

In this study, a series of isotropic compression tests were conducted to investigate yielding behaviour of intact, recompacted and reconstituted saturated loess specimens at various temperatures. Moreover, scanning electron microscope (SEM) images were used to explain structure effects on thermal softening.

2. Experimental studies

2.1 Test programme and apparatus

The principal objective of this study is to investigate effects of soil structure induced by different specimen preparation methods (intact, recompacted and reconstituted) on thermal softening of yield stress. To meet this objective, nine temperature-controlled isotropic compression tests were carried out. Three of them (I5, I23 and I50) were carried out on intact specimens at three different temperatures. With reference to the working condition of landfill cover and energy pile (Ng et al., 2014; Hao et al., 2017), the temperatures selected in this study are 5, 23 and 50°C. Three of them (C5, C23 and C50) on recompacted loess and another three tests (R5, R23 and R50) on reconstituted loess were also conducted at different temperatures (5, 23 and 50°C). All tests in this study were carried out at drained conditions with a constant total confining stress σ and zero pore water pressure u. The difference between them is effective confining stress, following the definition of Terzaghi (1943). Details of the

test program are summarized in Table 1. Moreover, SEM is also used to investigate the different microstructure of intact, recompacted and reconstituted specimens.

A temperature-controlled triaxial apparatus (Ng et al., 2016a) was utilised in the current study, as shown in Fig. 1. The temperature of soil specimen is controlled by a heating/cooling system, consisting of a water bath connected with a spiral copper tube installed between the inner cell and the outer cell. During a test, the water in the water bath is heated or cooled and then circulated in the spiral copper tube. Soil specimen is then heated or cooled by heat exchange. After reaching thermal equilibrium, the temperature fluctuation is less than 0.2°C. The total volume change of the specimen is measured by monitoring the change in the differential pressure between the water level inside the inner cell and that in the reference tube with a differential pressure transducer (DPT). During a test, a change in water level of the inner cell takes place only within the bottle neck, with a small diameter of 20 mm (Ng et al., 2002). Considering thermally induced volume change of soil specimen, rigorous calibration was carried out including the relationship between the DPT output voltage and the water level inside the inner cell at different pressures and temperatures, the thermal response of volume change measurement system as well as the rate of water diffusion through the membrane and drainage tubes at various pressures and temperatures. The accuracy of volume change measurement is about 0.03% volumetric strain for the specimen size used in this research (76 mm in diameter and 20 mm in height). More details of the test apparatus were reported by Ng et al. (2016a).

2.2 Soil type and specimen preparation

The soil studied in this research is loess sampled from Shaanxi Province, China. The index properties are summarized in Table 2. According to the Unified Soil Classification System (ASTM,

2011), the tested soil is classified as a clay of low plasticity (CL).

Intact block loess samples (0.25×0.25×0.25 m^3) were manually extracted using wooden cubic boxes at depth of 3.5 m, following the ASTM standard (ASTM, 2013). A cutter ring with 76 mm in diameter and 20 mm in height was used to obtain the intact specimens. The initial void ratio of intact loess was about 1.10 and the initial water content was 10.9%.

For recompacted specimens, static compaction was adopted. To produce a uniform specimen, the compaction of a 20 mm height triaxial specimen was conducted in 3 layers. Each layer was statically compressed at a fixed displacement rate of 1.0 mm/min. The compaction water content and void ratio were 10.9% and 1.15, respectively.

The reconstituted specimen was prepared from loess slurry at water content of 1.25 times of the liquid limit without air drying or oven drying (Barden et al., 1973). The slurry was consolidated at a vertical stress of 100 kPa inside a consolidometer (with 80 mm in diameter). A cut ring was used for retrieving specimens to the target size (76 mm in diameter and 20 mm in height). The initial void ratio of the reconstituted specimen was about 0.75.

2.3 Test procedures

After specimen preparation, each specimen was set up in the triaxial apparatus. For intact and recompacted specimens, saturation was firstly carried out by flushing with de-aired water for 24 hours. Fig. 2 shows the thermo-mechanical paths of all specimens after saturation. Similar to Tang et al. (2008) and Di Donna and Laloui (2015), each test consists of two stages (thermal loading and isotropic compression). The first stage is to change soil temperature to the target value. For the tests conducted under elevated temperature (I50, C50 and R50), this stage is to heat specimens to 50°C (A→B1). For

the tests at temperature lower than room temperature (I5, C5 and R5), this stage is to decrease soil temperature to 5°C (A→B2). For the specimens conducted under room temperature (I23, C23 and R23), the temperature keeps constant. In this study, two days are needed for temperature to reach the equilibrium state and for thermally induced excess pore water pressure to dissipate. The second stage is to isotropically compress all the soil specimens from 0 to 300 kPa (0-5-10-20-40-80-150-300) step by step at drained condition. Each step lasted for 24 hours to reach the equilibrium state (B1→C1; B2→C2; A→C3) (Maâtouk et al., 1995). The specific stress path of each isotropic compression test is summarized in Table 1.

3. Interpretations of experimental results

3.1 Effects of temperature and structure on isotropic compression behaviour

Fig. 3(a) shows thermal effects on the isotropic compression behaviour of intact loess. As expected, the void ratio of each specimen decreases with increasing confining stress. Each isotropic compression curve in the e-logp' plane consists of two approximately linear segments. The intersection of the two linear segments is determined as yield stress, following the method proposed by Sridharan et al. (1991). The yield stresses at different temperatures are determined and shown in the figure. The yield stresses are about 30, 25 and 20 kPa at 5, 23 and 50°C, respectively. It is evident that the yield stress of intact loess decreases with increasing temperature (i.e., thermal softening of yield stress). The observed thermal softening may be explained using double-layer theory. According to Israelachvili (2011), the inter-particle repulsive electrochemical force N_e is defined as the combination of double layer repulsion force and van der Waals attraction force:

$$N_e = 64GTce^{-\left(\frac{d}{\vartheta}\right)} - \frac{A_h R}{12d} \quad (1)$$

where G is the gas constant (8.314 $Jmol^{-1}K^{-1}$); T is temperature; c is pore-fluid concentration; e is the elementary charge (1.602×10^{-19} C); ϑ is the double layer thickness, which is insensitive to temperature change (Mitchell and Soga, 2005); d is the inter-particle distance; A_h is the Hamaker constant and R is the radius of spherical particles. On the left hand side of Equation (1), the first term $64GTce^{-\left(\frac{d}{\vartheta}\right)}$ represents the double layer repulsion force and the second term $\frac{A_h R}{12d}$ is the van der Waals attraction force. With increasing temperature, the double layer repulsion force increases and the van der Waals attraction force is almost constant. Hence, the value of N_e increases with increasing temperature. According to Lambe (1960), effective stress σ' is sum of the inter-particle normal contact force N per unit area and the inter-particle repulsive electrochemical force N_e per unit area. In this study, effective stress keeps unchanged during temperature change under drained condition. With increasing temperature, the inter-particle repulsive electrochemical force N_e increases. Hence, the inter-particle contact normal force N decreases. As a result, the ability for soil particles to resist rearrangement decreases and yield stress decreases with increasing temperature. Moreover, the plastic compressibility index λ is estimated using the slope of the second linear segment. It is found that λ of intact specimen is about 0.14 and temperature seems to have no influence on the plastic compressibility index. The observed thermal effects on yield stress and compressibility index of intact loess are consistent with experimental results in previous studies (Tidfors and Sällfors, 1989; Cekerevac and Laloui, 2004; Tang et al., 2008; Cui et al., 2000; Di Donna and Laloui, 2015).

Fig. 3(b) shows thermal effects on the isotropic compression behaviour of recompacted loess. The trend is qualitatively similar to that of intact specimen. For recompacted loess, the yield stresses are 13,

10 and 7 kPa at temperatures of 5, 23 and 50°C, respectively. At each temperature, the yield stress of recompacted specimen is smaller than that of intact one. The difference is mainly attributed to more resistant soil structure of intact specimen than recompacted one (Burland, 1990). In the SEM images shown in Fig. 4, the dots are clay particles. The small blocks with rough surface and diameters of a few micrometres are clay aggregates. The subangular blocks with diameters of a few tens of micrometres are silt grains. As evidenced by microstructural observations shown in Figs. 4(a) and 4(b), the structures of both intact and recompacted loess are dominated by silt particles. Clay particles in intact and recompacted specimens are gathering together and forming clay aggregates. This is confirmed by the pore size distributions of intact and recompacted loess from MIP test conducted by Ng et al. (2018). As investigated by Ng et al. (2018), bimodal pore size distributions with two distinct pore domains can be observed for intact and recompacted loess specimen. The two distinct pore domains are intra-aggregate pores and inter-aggregate pores (Delage et al., 1996; Romero et al., 2011; Ng et al., 2016c). Compared with recompacted specimen, there are more clay aggregates accumulating at inter-particle contacts in intact loess, as can be seen from the SEM images (Ng et al., 2016b; 2017). The inter-particle clay aggregates provide additional support to the silt grains and stiffen soil skeleton (Barden et al., 1973; Li et al., 2016). On the other hand, as can be obtained from Fig. 3(b), the plastic compressibility index λ of recompacted specimen is about 0.11, which is about 20% smaller than that of intact one. This is because, compared with recompacted loess, there are some extra-large pores with a diameter over 200 μm in intact loess (Ng et al., 2016a; Bai et al., 2014). These extra-large pores collapse easily after reaching initial yield stress, inducing a larger compressibility for intact loess. Besides, the inter-aggregate pores in intact specimen are larger than those in recompacted one, as evidenced by the PSD curves investigated by Ng et al. (2018). Moreover, from previous study

conducted by Ng et al. (2016a), the yield stresses of intact and recompacted specimens at temperatures of 5 and 50℃ can also be determined in a smaller stress range from 5 to 50 kPa, as shown in Fig. 3. The difference between the two replicates is less than 10%. This suggests that the laboratory data is reliable.

Fig. 3(c) shows thermal effects on the isotropic compression behaviour of reconstituted loess. The trend is also qualitatively similar to those of intact and recompacted loess. The yield stresses of reconstituted loess at temperatures of 5, 23 and 50°C are determined as 90, 68 and 44 kPa, respectively. The reconstituted specimen was prepared in a one-dimensional consolidometer with a consolidation stress (i.e., vertical effective stress) of 100 kPa. For such a normally consolidated reconstituted specimen, the coefficient of later stress (K0) was far less than 1 (Feda et al., 1995). The maximum mean effective stress is therefore less than 100 kPa during the specimen preparation. Hence, the yielding stress determined from isotropic compression tests is below 100 kPa. The yield stress of reconstituted specimen at a given temperature is much larger than those of intact and recompacted loess. It is because the initial density of the reconstituted specimen is much larger. If the reconstituted specimen had been prepared to a density equal to that of the intact specimen, the yield stress of the reconstituted specimen should be smaller than that of the intact one. This is because soil structure can restrain the deformation and the soil structure of reconstituted specimen is considered to be fully destroyed during preparation (Burland et al., 1990; Liu and Carter, 2002; Hong et al., 2012). The plastic compressibility index λ of intact specimen is about 0.08, which is the smallest compared with those of reconstituted and recompacted specimens. This is consistent with the results of previous studies (Balasubramanian and Hwang, 1980; Burland, 1990; Liu and Carter, 2002), which reveals that the compressibility of reconstituted specimen is smaller than that of structured specimen as the

structure of is fully destroyed during the preparation. As evidenced by the SEM image shown in Fig. 4(c), the soil structure of reconstituted specimen is generally homogeneous and silt particles with clay matrix rather than clay aggregates between them can be identified clearly.

3.2 Influence of soil structure on thermal softening

According to previous studies (Burland, 1990; Liu and Carter, 2002), the behaviour of reconstituted soil can be considered as a reference. The isotropic compression behaviour of reconstituted and structured soils (i.e., intact and recompacted specimens) can be linked as follow:

$$e = e^* + \Delta e \tag{2}$$

where e is the void ratio of structured soil at a given stress state; e^* is the void ratio of the corresponding reconstituted soil at the same stress state; Δe, the additional void ratio, is the difference in void ratio between the tested soil and the reconstituted one. Δe at the initial yield stress of a structured soil is defined as Δe_i to quantify the structure of intact, recompacted and reconstituted specimens (Liu and Carter, 2002). The values of Δe_i are 0.27, 0.25 and 0 for intact, recompacted and reconstituted specimen, respectively. A larger Δe_i suggests a more resistant soil structure.

Fig. 5(a) shows the relationship between $p_c(T)$ and T for intact, recompacted and reconstituted specimens. In order to determine thermal softening of yield stress for each type of specimens (intact, recompacted and reconstituted), yield stress at a given temperature is normalized by that at a reference temperature (5°C). According to the theoretical equation derived by Zhou and Ng (2018), the normalized yield stress $p_c(T)/p_c(T_0)$ can be calculated using the equation as follows:

$$\frac{p_c(T)}{p_c(T_0)} = \exp\left(\frac{v(T)-v(T_0)}{\lambda-\kappa}\right) \quad (3)$$

where $v(T)$ and $v(T_0)$ are the specific volumes of a normally consolidated soil at T and T_0, respectively, under the same stress condition; λ is the plastic compressibility index and κ is the elastic compressibility index. All of these four parameters are obtained based on compression lines shown in Fig. 3. The relationship between normalized yield stress and normalized temperature is shown in Fig. 5(b). According to Laloui and Cekerevac (2003), the relationship between yield stress and temperature can be expressed by the following equation:

$$\frac{p_c(T)}{p_c(T_0)} = 1 - \gamma_T \log\left(\frac{T}{T_0}\right) \quad (4)$$

where γ_T is a material parameter describing the evolution of yield stress with temperature. For intact, recompacted and reconstituted loess specimens, the values of γ_T is found to be 0.280, 0.393 and 0.608, respectively. In other words, a smaller material parameter γ_T represents a more resistant structure to thermal softening. It is clear that the behaviour of recompacted loess is more similar to that of intact loess, rather to that of reconstituted loess. This is consistent with the SEM images shown in Fig. 4, which clearly reveal that the microstructure of intact and recompacted loess are similar. Moreover, the thermal softening of yield stress is the least significant for intact loess in the temperature range considered. This is because in intact loess, clay particles form aggregates and accumulates at the inter-particle contacts, as shown in Fig. 4(a). These aggregates stabilize the structure of intact loess as they enlarge the inter-particle contact areas and hence stabilize soil skeleton (Ng et al., 2016b; 2017). On the other hand, the thermal softening of yield stress of reconstituted specimen is the most significant, mainly attributed to its microstructure. For reconstituted loess, silt particles are dominated but clay particles float on the surface of silt particles, as shown in Fig. 4(c). Without the stabilisation effects of clay aggregates on inter-particle contacts, the thermal softening of yield stress is the most

severe in reconstituted loess. The observed phenomenon can be used to explain experimental results conducted by Ng et al. (2018). According to existing thermo-mechanical models (Cui et al., 2000; Abuel-Naga et al., 2007; Laloui and Cekerevac, 2008; Yao and Zhou, 2012; Zhou and Ng, 2018), there is a positive relationship between incremental volumetric strain and incremental yield stress. Therefore, within the same temperature range, thermally induced plastic volumetric strain of reconstituted loess is larger than those of intact and recompacted loess.

4. Conclusions

This study is the first study to investigate the effects of soil structure induced by specimen preparation methods on thermal softening of yield stress. Experimental results show that for saturated intact, recompacted and reconstituted loess specimens, yield stresses all decrease with increasing temperature (i.e., thermal softening of yield stress). This is probably because with increasing temperature, the inter-particle repulsive electrochemical force between soil particles increases, resulting in a smaller inter-particle contact normal force.

When temperature increases from 5 to 50°C, the yield stresses of the intact, recompacted and reconstituted specimens decreased by about 33%, 46% and 51%, respectively. It is evident that soil structure has a significant influence on thermal softening of yield stress. The most resistant structure to thermal softening of intact specimen is because the clay aggregates accumulated at the inter-particle contacts in intact specimen stiffen the soil skeleton, as evidenced by SEM images. Reconstitute specimen has the least resistant structure to thermal softening. This is because clay particles in reconstituted specimen float on the grain surfaces rather than at inter-particle contacts. The experimental results can be used to explain different thermo-mechanical behaviour of soil specimens

with various soil structures. Moreover, the results are beneficial to verify constitutive models considering the effects of soil structure on the thermal behaviour.

Acknowledgements

The authors would like to thank the Research Grants Council of the Hong Kong Special Administrative Region (HKSAR) for their financial supports from the research grants 616812 and 16216116. In addition, Projects 51509041 and 41902271 supported by the National Natural Science Foundation of China is grateful acknowledged.

References

Abuel-Naga, H., Bergado, D.T., Bouazza, A., Ramana, G.V., 2007. Volume change behaviour of saturated clays under drained heating conditions: experimental results and constitutive modelling. Canadian Geotechnical Journal 44(8), 942-956.

ASTM, 2011. Standard practice for classification of soils for engineering purposes (Unified Soil Classification System), ASTM standard D2487, American Society for Testing and Materials, West Conshohocken.

ASTM, 2013. Standard Practices for Obtaining Intact Block (Cubical and Cylindrical) Samples of Soils, ASTM standard D7015, American Society for Testing and Materials, West Conshohocken.

Balasubramanian, A.S., Hwang, Z.M., 1980. Yielding of weathered Bankok clay. Soils and Foundations 20(2), 1-15.

Bai, X.H., Ma, F.L., Wang, M., Jia, J.G., 2014. Micro-structure and collapsibility of loess in China. In Geomechanics from Micro to Macro, 1303-1308.

Barden, L., McGown, A., Collins, K., 1973. The collapse mechanism in partly saturated soil. Engineering Geology 7(1), 49-60.

Burland, J.B., 1990. On the compressibility and shear strength of natural clays. Géotechnique 40(3), 329-378.

Cekerevac. C., Laloui. L., 2004. Experimental study of thermal effects on the mechanical behaviour of a clay. International Journal for Numerical and Analytical Methods in Geomechanics 28(3), 209-228.

Cui, Y.J., Sultan, N., Delage, P., 2000. A thermomechanical model for saturated clays. Canadian Geotechnical Journal 37(3), 607-620.

Delage, P., Audiguier, M., Cui, Y.J., Howat, M.D., 1996. Microstructure of a compacted silt. Canadian Geotechnical Journal 33(1), 150-158.

Di Donna, A., Laloui, L., 2015. Response of soil subjected to thermal cyclic loading: experimental and constitutive study. Engineering Geology 190, 65-76.

Feda, J., Bohac, J., Herle, I., 1995. K0-compression of reconstituted loess and sand with stress perturbations. Soils and Foundations 35(3), 97-104.

Gens, A., 2010. Soil–environment interactions in geotechnical engineering. Géotechnique 60(1), 3-74.

Hao, Z., Sun, M., Ducoste, J., Barlaz, M., 2017. A Model to Describe Heat Generation and Accumulation at Municipal Solid Waste Landfills. Geotechnical Frontiers 281-288.

Hong, Z.S., Zeng, L.L., Cui, Y.J., Cai, Y.Q., Lin, C., 2012. Compression behaviour of natural and reconstituted clays. Géotechnique 62(4), 291-301.

Israelachvili, J.N., 2011. Intermolecular and surface forces: revised third edition, Academic press.

Lambe, T.W., 1960. A mechanistic picture of shear strength in clay. Proccedings ASCE Research conference on shear strength of cohesive soils, Boulder, Colorado, 555-580.

Laloui, L., Cekerevac, C., 2003. Thermo-plasticity of clays: An isotropic yield mechanism. Computers and Geotechnics 30(8), 649-660.

Laloui, L., Cekerevac, C., 2008. Non-isothermal plasticity model for cyclic behaviour of soils. International Journal for Numerical and Analytical Methods in Geomechanics 32(5), 437-460.

Li, P., Vanapalli, S., Li, T.L., 2016 Review of collapse triggering mechanism of collapsible soils due to wetting. Journal of Rock Mechanics and Geotechnical Engineering 8(2), 256-274.

Liu, M.D., Carter, J.P., 2002. A structured Cam Clay model. Canadian Geotechnical Journal 39(6), 1313-1332.

Maâtouk, A., Leroueil, S., La Rochelle, P., 1995. Yielding and critical state of a collapsible unsaturated silty soil. Géotechnique 45(3), 465-477.

Marshall, T.J., Holmes, J.W., 1979. Soil Physics, Cambridge University Press, Cambridge.

Mitchell, J.K., Soga, K., 2005. Fundamentals of soil behavior, 3rd edn. New York, NY, USA: John Wiley & Sons.

Ng, C.W.W., Cheng, Q., Zhou, C., Alonso, E.E., 2016a. Volume changes of an unsaturated clay during heating and cooling. Géotechnique Letters 6(3), 192-198.

Ng, C.W.W., Kaewsong, R., Zhou, C., Alonso, E.E., 2017. Small strain shear moduli of unsaturated natural and compacted loess. Géotechnique 67(7), 646-651.

Ng, C.W.W., Mu, Q.Y., Zhou, C., 2016b. Effects of soil structure on the shear behaviour of an unsaturated loess at different suctions and temperatures. Canadian Geotechnical Journal 54(2), 270-279.

Ng, C.W.W., Mu, Q.Y., Zhou, C., 2018. Effects of specimen preparation method on the volume change of clay under cyclic thermal loads. Géotechnique 69(2), 146-150.

Ng, C.W.W., Sadeghi, H., Hossen, S.K.B., Chiu, C.F., Alonso, E.E., Baghbanrezvan, S., 2016c. Water retention and volumetric characteristics of intact and re-compacted loess. Canadian Geotechnical Journal 53 (8), 1258-1269.

Ng, C.W.W., Shi, C., Gunawan, A., Laloui, L., 2014. Centrifuge modelling of energy piles subjected to heating and cooling cycles in clay. Geotechnique letters 4(4), 310-316.

Ng, C.W.W., Zhan, L.T., Cui, Y.J., 2002. A new simple system for measuring volume changes in unsaturated soils. Canadian Geotechnical Journal 39(3), 757-764.

Romero, E., Simms, P.H., 2008. Microstructure investigation in unsaturated soils: a review with special attention to contribution of mercury intrusion porosimetry and environmental scanning electron microscopy. Geotechnical and Geological Engineering 26, 705-727.

Romero, E., Della Vecchia, G., Jommi, C., 2011. An insight into the water retention properties of compacted clayey soils. Géotechnique 61 (4), 313-328.

Sridharan, A., Abraham, B.M., Jose, B.T., 1991. Improved technique for estimation of yield stress. Géotechnique 41(2), 263-268.

Sridharan, A., Nagaraj, H.B., 2000. Compressibility behavior of remolded, fine-grained soils and correlation with index properties. Canadian Geotechnical Journal 37(3), 712-722.

Tang, A.M., Cui, Y.J., Barnel, N., 2008. Thermo-mechanical behaviour of a compacted swelling clay. Géotechnique 58(1), 45-54.

Terzaghi, K., 1943. Theoretical Soil Mechanics, John Wiley and Sons, New York.

Tidfors, M., Sällfors, S., 1989. Temperature effect on preconsolidation pressure. Geotechnical Testing

Journal 12(1), 93-97.

Xiong, Y.L., Yang, Q.L., Zhang, S., Ye, G.L., Liu, G.B., Zheng, R.Y., Zhang, F., 2018. Thermo-elastoplastic Model for Soft Rock Considering Effects of Structure and Overconsolidation. Rock Mechanics and Rock Engineering 51(12), 3771-3784.

Yao, Y.P., Zhou, A.N., 2013. Non-isothermal unified hardening model: a thermo-elasto-plastic model for clays. Géotechnique 63(15), 1328-1345.

Zhou, C., Ng, C.W.W., 2018. A new thermo-mechanical model for structured soil. Géotechnique 68(12), 1109-1115.

List of tables

List of figures

Table 1 Details of temperature-controlled isotropic compression tests

Test ID	Specimen type	Temperature (°C)	Initial void ratio	Void ratio after saturation	Stress path (see Fig. 1)
R50	Reconstituted	50	0.75	0.75	A→B1→C1
R23	Reconstituted	23	0.75	0.75	A→C3
R5	Reconstituted	5	0.75	0.75	A→B2→C2
C50	Recompacted	50	1.15	1.16	A→B1→C1
			1.17	1.17	
C23	Recompacted	23	1.15	1.15	A→C3
C5	Recompacted	5	1.15	1.15	A→B2→C2
			1.17	1.17	
I50	Intact	50	1.12	1.13	A→B1→C1
			1.12	1.13	
I23	Intact	23	1.11	1.12	A→C3
I5	Intact	5	1.11	1.11	A→B2→C2
			1.14	1.15	

Table 2 Index properties of the tested loess

Property	Value
Specific gravity	2.69
Sand content (%)	0.1
Silt content (%)	71.9
Clay content (%)	28.0
Liquid limit (%)	36
Plastic limit (%)	19
Plasticity index (%)	17

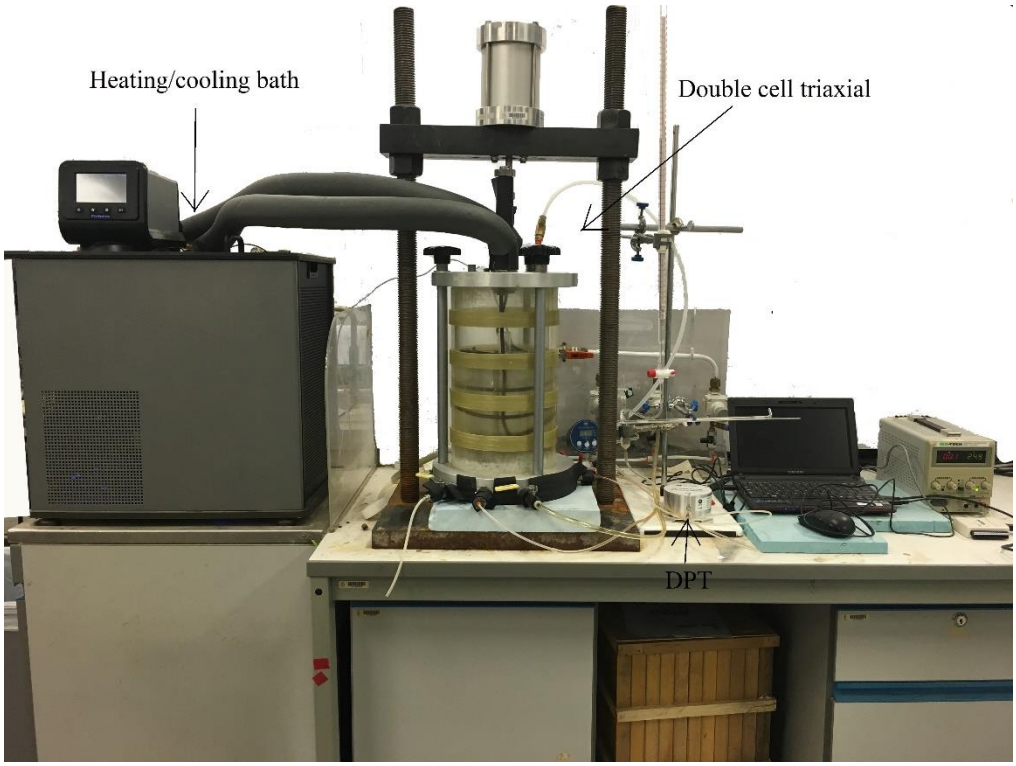

Fig. 1 Photograph of the temperature-controlled triaxial apparatus

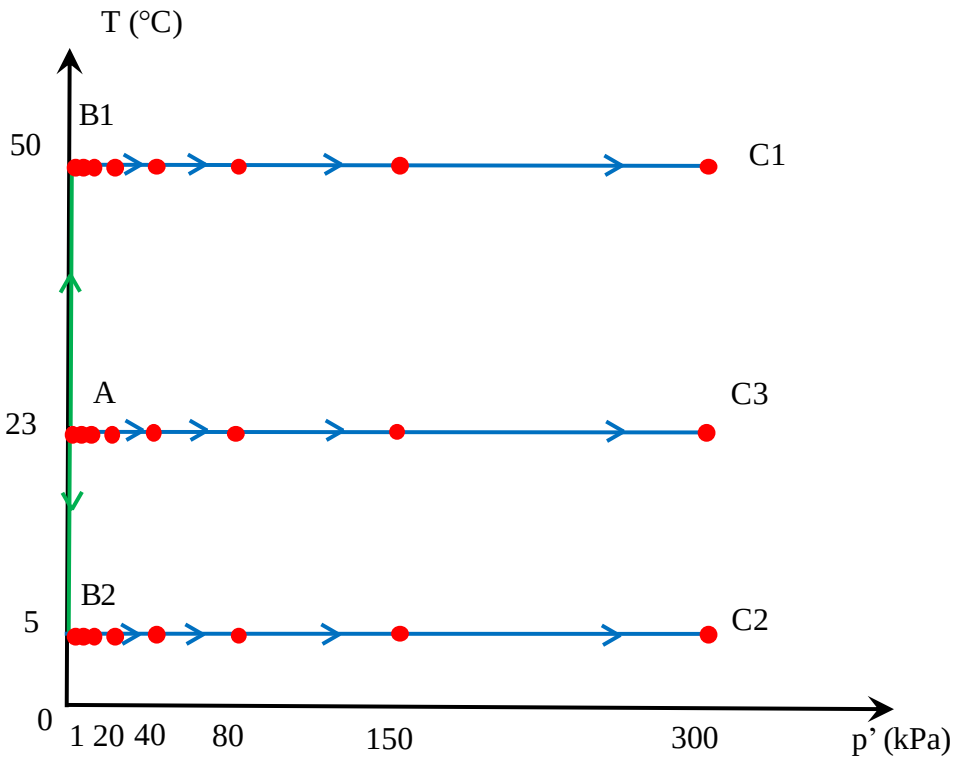

Fig. 2 Thermo-mechanical path of each specimen

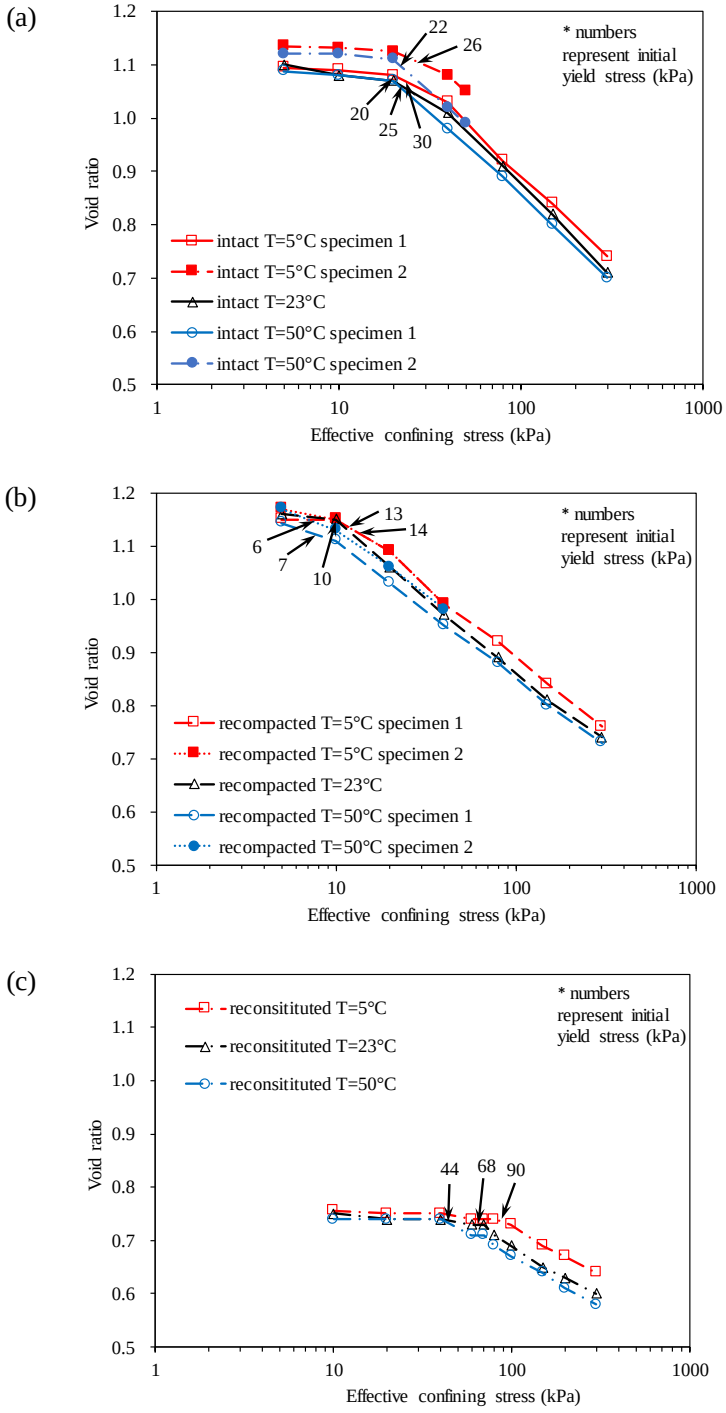

Fig. 3 Thermal effects on isotropic compression behaviour of (a) intact loess, (b) recompacted loess and (c) reconstituted loess

(a)

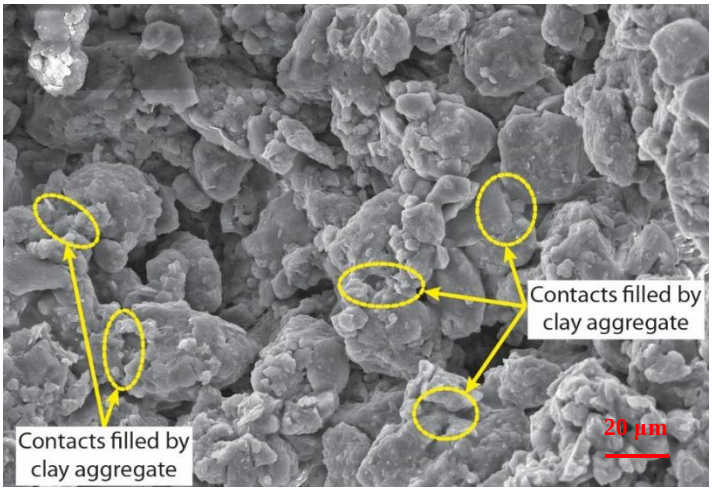

(b)

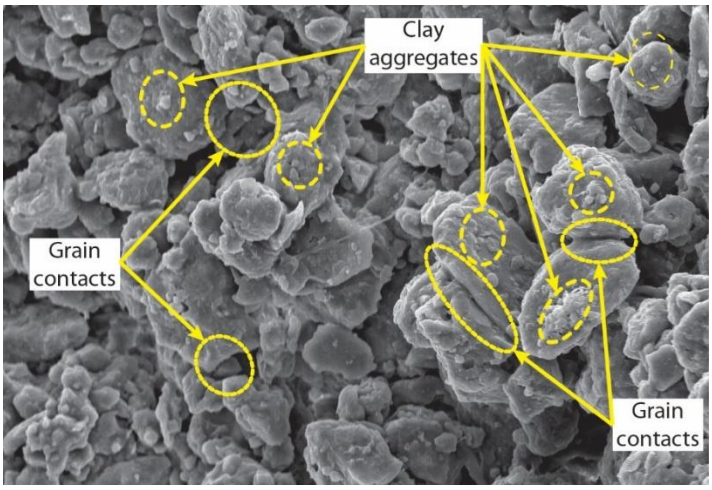

(c)

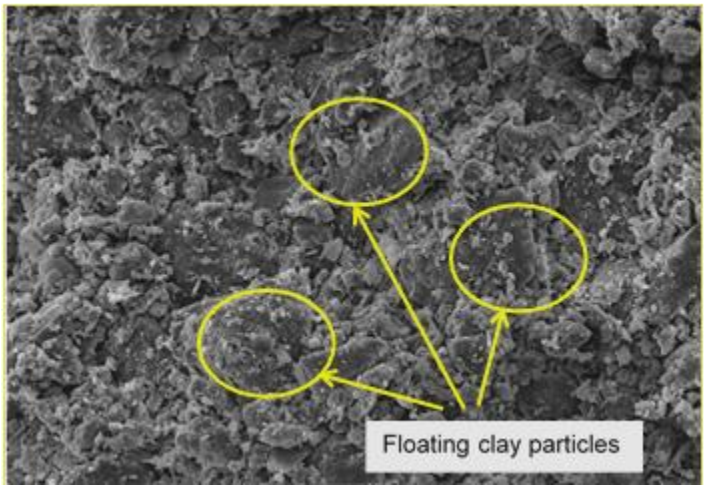

Fig. 4 SEM images of (a) intact loess, (b) recompacted loess and (c) reconstituted loess (after Ng et al., 2016b)

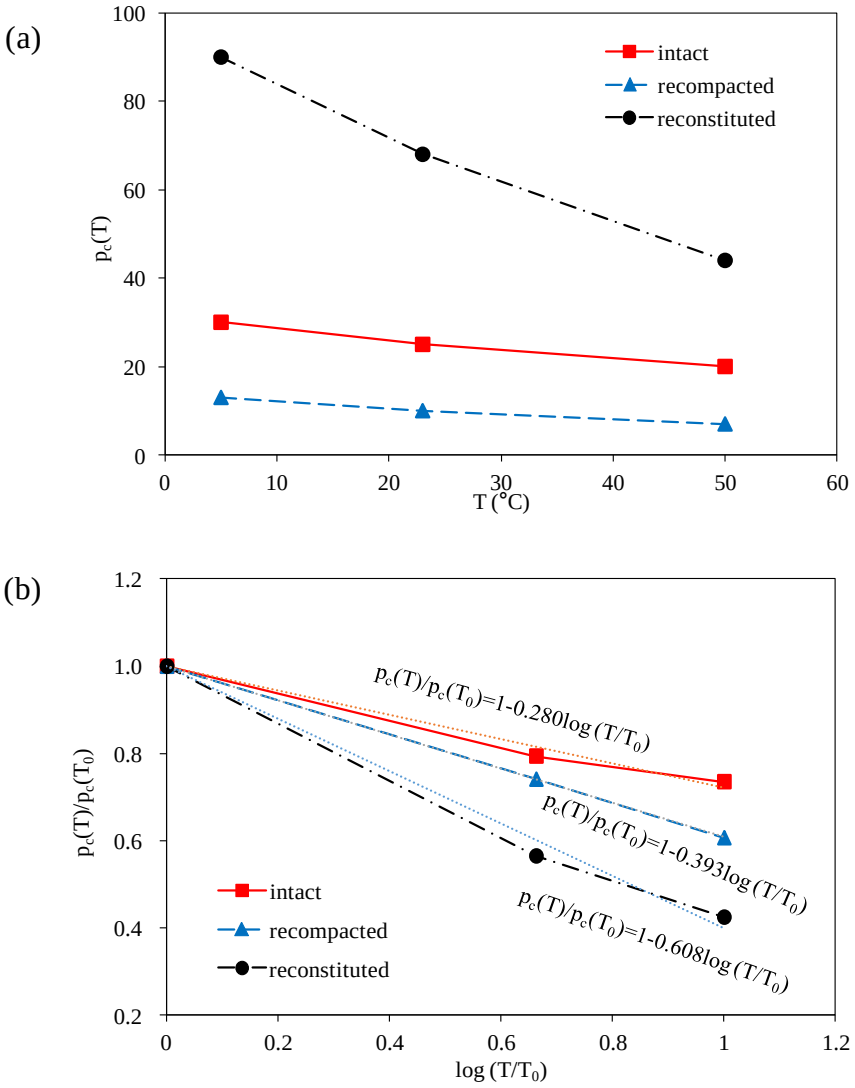

Fig. 5 Effects of soil structure on thermal softening of yield stress